Research Journal of Applied Sciences, Engineering and Technology 8(12): 1396-1403, 2014
DOI:10.19026/rjaset.8.1113
ISSN: 2040-7459; e-ISSN: 2040-7467

Submitted: April 29, 2014 Accepted: May 25, 2014 Published: September 25, 2014

Research Article

An Efficient Steganalytic Algorithm based on Contourlet with GLCM

[1]T.J. Benedict Jose and [2]P. Eswaran
[1]Department of Computer Science, Manonmaniam Sundaranar University, Tirunelveli, India
[2]Department of Computer Science, Alagappa University, Karaikudi, India

Abstract: Steganalysis is a technique to detect the hidden embedded information in the provided data. This study proposes a novel steganalytic algorithm which distinguishes between the normal and the stego image. III level contourlet is exploited in this study. Contourlet is known for its ability to capture the intrinsic geometrical structure of an image. Here, the lowest frequency component of each level is obtained. The pixel distance is taken as 1 and the directions considered are 0, 45, 90 and 180°, respectively. Finally, Support Vector Machine (SVM) is used as the classifier to differentiate between the normal and the stego image. This steganalytic system is tested with DWT, Ridgelet, Contourlet, Curvelet, Bandelet and Shearlet. All these were tested in the aspects of first order, Run length and Gray-Level Co-occurrence Matrix (GLCM) features. Among all these, Contourlet with GLCM shows the maximum accuracy of 98.79% and has the lowest misclassification rate of 1.21 and are presented in graphs.

Keywords: Contourlet, first order, GLCM, run length, steganalysis, SVM

INTRODUCTION

Steganography is the art of embedding any secret information within an object. With the advent of internet, the transfer of image, video and other data files made simpler and is done by most of the population. While such file transfer, a conversion between analogues to digital takes place.

Steganography hits the scene at this point of time. This steganography was paid much attention around 2001. There are several hundreds of stego systems available. This method of message hiding can be done in JPEG, GIF and BMP images. However, JPEG is the most common medium that is used for steganography.

Every stego system must have a cover medium, an embedding algorithm, a secret message and a secret key. The cover medium can be anything such as an image, an audio file, video or any digital file. Here, the image with secret message, key and the cover medium are passed into the embedding algorithm.

The outcome of this is a stego image, which cannot be claimed that something has been embedded in the image, with naked eye. A perfect stego image looks clear such that doubt of the presence of any secret message is avoided. Steganalysis is the science of detecting secret communications. The steganalytic algorithm is said to be successful, when it perfectly differentiates whether the image contains secret information or not.

The goal of steganalysis is to discover the information that is hidden, within the cover object. This analysis has to be done without any prior knowledge of the secret key being used to embed and also the embedding algorithm.

In fine, the process of embedding a secret message into a cover medium is steganography and the science of identifying the presence of secret message is steganalysis.

LITERATURE REVIEW

Westfeld and Pfitzmann (2000) has presented a method that is based on statistical analysis of Pairs of Values, which are exchanged when the message is embedded. This method is known as χ^2 attack which makes use of correlations between input and output measured by the χ^2 test. The χ^2-attack was originally proposed by Vaudenay (1996) as an attack on the Data Encryption Standard (DES). This can be applied to many embedding paradigms rather than the LSB embedding.

Westfeld (2001) has presented a new steganographic algorithm named F5, which emphasized that the embedding density should remain the same throughout. This resulted in a high steganographic capacity with high efficiency, since more number of bits can be embedded per change.

In the work proposed by Kaur *et al*. (2011), a DCT based watermarking scheme with high resistivity over image processing attacks such as JPEG compression, noise, rotation and translation, is proposed. Here, the watermark is embedded in the mid-frequency band of

Corresponding Author: T.J. Benedict Jose, Department of Computer Science, Manonmaniam Sundaranar University, Tirunelveli, India

the DCT blocks carrying low frequency components. A work is proposed by Fontaine and Galand (2009) attempts to lock maximal number of positions, Lagrange interpolation is incorporated. This is followed by the algorithm based on Guruswami-Sudan list decoding.

Another work that is mainly meant to detect between the normal and stego images by exploiting SVM, in which a model is obtained by training a dataset and then the obtained model is used over the testing dataset, to predict information (Chang and Lin, 2001).

Kundur and Hatzinakos (1998) proposed a novel and a robust technique for digital watermarking for still images on the basis of multi-resolution wavelet fusion. The work presented by Schönfeld and Winkler (2007), deals with the strategies to reduce the complexities in embedding on the basis of syndrome coding and at the same time, by maintaining the embedding efficiency constant. This study proposes different approaches to reduce embedding complexity by concentrating both on syndrome coding based on parity check matrix and generator polynomial.

Huang *et al*. (2012) has presented a new channel rule for JPEG steganography, which reduced the detection capability of several JPEG steganalyzers. The efficiency of this channel is tested with four different JPEG steganalyzer.

Farid (2001) has implemented a detection scheme, which is applicable to all steganographic schemes. This is made possible by providing proper training of original and stego images to databases. Farid (2001) made use of optimal linear predictor to have wavelet coefficients, based on which the first four moment of the distribution of prediction error is calculated. Then a threshold is found out by using Fisher's linear discriminant statistical clustering, to identify between the stego and the normal images.

Fridrich *et al*. (2003) have broken the F5, which is a steganographic algorithm, by estimating the value of 'β', that can consequently be turned into an estimate of the secret embedded message. After getting the baseline histograms, the modified non-zero non DC coefficients are determined, in order to arrive at 'β', which minimizes the least square error between the stego image histogram and the histograms obtained by embedding a message that paves way to extract 'β, modifications. Fridrich (2004) has stated that decompressed JPEG images should be avoided as cover medium for spatial steganography, such as the LSB embedding or so. Selection of cover images is also given importance in the work done by Fridrich (2004). Selection of cover images has its impact over the stego system and security. Images with low number of colors, computer art are needed to be excluded, since they cannot serve as better cover images.

Fridrich *et al*. (2004) investigated the statistical detect-ability of several steganographic methods, by determining maximal relative payload, at which the methods would be undetectable statistically. Dey *et al*. (2011) has proposed a wavelet based steganographic technique for color images. The true color cover image and the secret images are decomposed into three separate color planes namely R, G and B. Each plane is decomposed into four sub-bands using DWT. Each color plane of the secret image is hidden by alpha blending technique in the corresponding sub-bands of the respective color planes of the original images. The secret image is dispersed within the original image with respect to the alpha value.

Aura (1996) suggests that gray-scale images are the best choice for cover images. The work proposed by Jose and Eswaran (2013), presents a steganalytic algorithm that differentiates between the stego and the normal image. This is done by calculating residual values along 0, 45, 90 and 135°, respectively and it proves 90% accuracy. Zhu *et al*. (1998) a unified approach to digital watermarking of images and video based on two and three dimensional DWT.

METHODOLOGY

SVM classifier: We use SVM classifier for finding the difference between the training and the testing features. Some of the reasons for why SVM Classifier is employed are as follows:

- By introducing the kernel, SVMs gain flexibility in the choice of the form of the threshold separating solvent from insolvent companies, which needs not be linear and even needs not have the same functional form for all data, since its function is non-parametric and operates locally. As a consequence they can work with financial ratios, which show a non-monotone relation to the score and to the probability of default, or which are non-linearly dependent and this without needing any specific work on each non-monotone variable.
- Since the kernel implicitly contains a non-linear transformation, no assumptions about the functional form of the transformation, which makes data linearly separable, is necessary. The transformation occurs implicitly on a robust theoretical basis and human expertise judgment beforehand is not needed.
- SVMs provide a good out-of-sample generalization, if the parameters C and r (in the case of a Gaussian kernel) are appropriately chosen. This means that, by choosing an appropriate generalization grade, SVMs can be robust, even when the training sample has some bias.
- SVMs deliver a unique solution, since the optimality problem is convex. This is an advantage

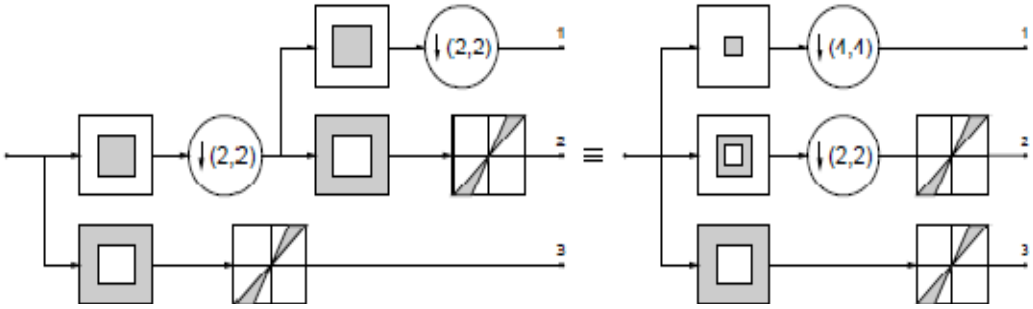

Fig. 1: Contourlet transform with 2 levels of multi-scale decomposition

compared to Neural Networks, which have multiple solutions associated with local minima and for this reason may not be robust over different samples.

- With the choice of an appropriate kernel, such as the Gaussian kernel, one can put more stress on the similarity between companies, because the more similar the financial structure of two companies is, the higher is the value of the kernel.

Thus when classifying a new company, the values of its financial ratios are compared with the ones of the support vectors of the training sample, which is more similar to this new company. This company is then classified according to with which group it has the greatest similarity (Auria and Moro, 2008).

Contourlet: The contourlet transform consists of two major stages: the subband decomposition and the directional transform. At the first stage, Laplacian Pyramid (LP) is used to decompose the image into subbands and then the second one is a Directional Filter Bank (DFB) which is used to analyze each detail image (Jassim, 2010).

Multi-resolution analysis: In the followings and for simplicity, the case with orthogonal filters, which lead to tight frames will be considered only. Multi-resolution analysis is divided into the following two types of analysis and is given below.

Multi-scale analysis: This is the multi-resolution analysis for the LP, which is similar to the one for wavelets. Suppose that the LP in the contourlet filter bank uses orthogonal filters and down sampling by 2 in each dimension as shown in Fig. 1, which is presented in Eq. (1):

$$M = diag(2,2) \quad (1)$$

Under certain regularity conditions, the lowpass synthesis filter G in the iterated LP uniquely defines a unique scaling function $\varphi(t) \epsilon L_2 R^2$ that satisfies the following two-scale equation (Jose and Eswaran, 2013):

$$\sqrt{2}\varphi(t) = 2\sum_{n\epsilon Z^2} g[n]\varphi(2t-n) \quad (2)$$

where, g [n] is the impulse response of the low pass synthesis filter G:

$$\text{Let } {}^{\varphi}{}_{j,n} = 2^{-j}\varphi\left(\frac{t-2^j n}{2^j}\right), \text{j}\in Z, n \in Z^2 \quad (3)$$

Then the family $\{\varphi_{j,n}\} n \in Z^2$ is an orthonormal basis for an approximation subspace V_j at the scale 2^j. Furthermore, provides a sequence of multi-resolution nested subspaces....$V_2 \Subset V_1 \Subset V_0 \Subset V_{-1} \Subset V_{-2}$..., where V_j is associated with a uniform grid of intervals 2j 2j that characterizes image approximation at scale 2j.

The difference images in the LP contain the details necessary to increase the resolution between two consecutive approximation subspaces. Therefore, the difference images live in a subspace W_j that is the orthogonal complement of V_j in V_{j-1}, as shown in (Fig. 2), or:

$$V_{j-1=}V_j \oplus W_j \quad (4)$$

It is believed that the LP can be considered as an oversampled filter bank where each polyphase component of the difference image d [n] in Fig. 1, together with the coarse image c [n], comes from a separate filter bank channel with the same sampling matrix M = diag (2, 2).

Let F_i (z), $0 \le i \le 3$ be the synthesis filters for these polyphase components. These are highpass filters. As for wavelets, a continuous function $\Psi^{(i)}(t)$, can be associated with each of these filters, where,

$$\sqrt{2}\,\Psi^{(i)}(t) = 2\sum_{n\epsilon Z^2} f_1[n]{}^{\varphi}(2t-n) \quad (5)$$

where, f_i [n] is the impulse response of the highpass synthesis filter F_i (z).

So, letting $\Psi^{(i)}(t)$ in (4) be in the form:

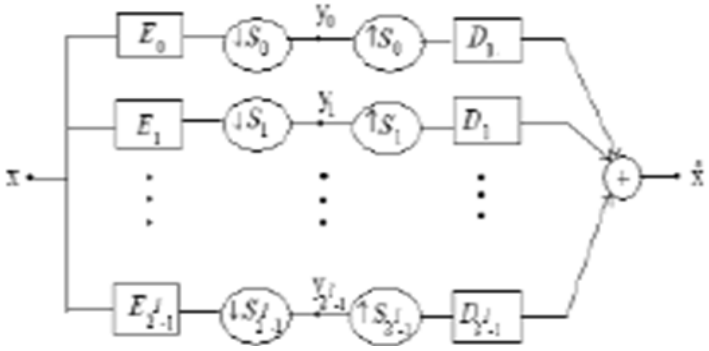

Fig. 2: Multichannel view of a l-level tree structured DFB

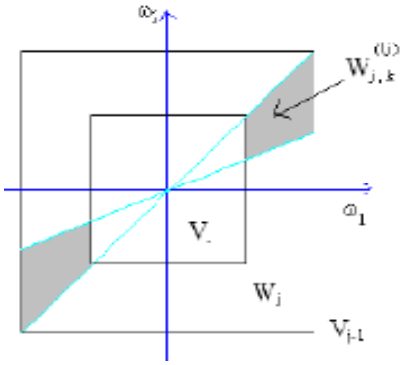

Fig. 3: Multi-scale and multi-direction subspaces

$$\Psi_{j,n}^{(i)}(t) = 2^{-j}\Psi^{(t)}\left(\frac{t-2^{j}n}{2^{j}}\right), j \in Z, n \in Z^2 \quad (6)$$

Then, for scale 2_j, $\left\{\Psi_{j,n}^{(i)}\right\}$ $0 \le i \le 3$, $n \in Z^2$ is tight frame for *Wj*. For all scales, $\left\{\Psi_{j,n}^{(i)}\right\}$ $j \in Z^2$ $0 \le i \le 3$, $n \in Z^2$ is a tight frame for L_2 (R^2). In both cases, the frame bounds are equal to 1. Since *Wj* is generated by four kernel functions (similar to multi-wavelets), in general it is not a shift-invariant subspace. Nevertheless, a shift-invariant subspace can be simulated by denoting:

$$\mu_{j,2n+k_i}(t) = \Psi_{j,n}^{(i)}(t), 0 \le i \le 3 \quad (7)$$

where, k_i are the coset representatives for down sampling by 2 in each dimension, i.e.:

$$k0 = (0, 0)\ T,\ k1 = (1, 0)\ T,\ k2 = (0, 1)\ T,\ k3 = (1, 1) \quad (8)$$

with this notation, the family $\{\mu_{j,n}\}, n \in Z^2$ associated to a uniform grid of intervals $2^{j-1} \times 2^{j-1}$ on R^2 provides a tight frame for W_j.

Multi-direction analysis: Using multi-rate identities Aura (1996), it is instructive to view an l-level tree-structured DFB equivalently as a 2^l parallel channel filter bank, as in Fig. 2, with equivalent analysis filters, synthesis filters and overall sampling matrices. The equivalent directional analysis filters are denoted as $E_k^{(l)}, 0 \le k \le 2^l$ and the directional synthesis filters as $D_k^{(l)}, 0 \le k < 2^l$, which corresponds to the subbands.

The corresponding overall sampling matrices S_k^l are proved to have the following diagonal forms (Aura, 1996) and are provided in below given equation:

$$S_k^l = \begin{cases} \begin{bmatrix} 2^{l-1} & 0 \\ 0 & 2 \end{bmatrix} \\ \begin{bmatrix} 2 & 0 \\ 0 & 2^{l-1} \end{bmatrix} \end{cases} \quad (9)$$

Which means sampling is separable. The two sets correspond to the mostly horizontal and mostly vertical set of directions, respectively. From the equivalent parallel view of the DFB, it can be seen that the family and shown in Eq. (10):

$$\left\{d_k^{(l)}\left[n - S_k^{(l)}m\right]\right\} 0 \le k < 2^l, m \in Z^2 \quad (10)$$

Obtained by translating the impulse responses of the equivalent synthesis filters $D_k^{(l)}$ over the sampling lattices by $S_k^{(l)}$, provides a basis for discrete signals in L2 (z^2).

This basis exhibits both directional and localization properties. In the iterated contourlet filter bank, the discrete basis (9) of the DFB can be regarded as a change of basis for the continuous-domain subspaces from the multi-scale analysis of the previous LP stage. Suppose that the DFB in the contourlet filter bank utilizes orthogonal filters and when such DFB is applied to the difference image (detail) subspaces then the resulting detail directional subspaces $W_{j,k}^{(l)}$ in the frequency domain will be as illustrated in Fig. 3.

Implementation: This study follows the below mentioned steps, in order to find if an image has got

any secret message embedded within. Initially, the entire system is trained, in order to gain knowledge about the stego image.

Training is done by applying 3 level contourlet transform in the image. For each level, the component which has got the lowest frequency value is picked out. This step is followed by obtaining the parameters such as pixel distance and direction.

This study considers that the pixel distance is 1and the directions 0, 45, 90 and 180, respectively are taken into account. The occurrence of each pixel pair is found out and these are stored in an array.

This array is the so called co-occurrence matrix and the mean value is applied to the co-occurrence matrix. These mean values are fed into the SVM classifier for knowledge gaining. In the testing phase, the user is prompted to select the image that needs to be tested.

Then the 3 level contourlet is applied over the image. The lowest frequency component is captured on each level and the pixel distance and directions are obtained.

The occurrence of each pixel pair is picked out and placed in an array. The mean value of all images is applied over this array.

Finally, the gained value of the training images and the mean value of the testing image is passed into SVM, in order to classify between the normal and the stego image. This study proves 98.79% accuracy. Most of the time, this study correctly classifies between the normal and the stego image.

Training phase:

- The training images are obtained.
- The below steps are applied for all images in the training folder:
  - Three level contourlet transform is applied on the image.
  - The low frequency component is obtained on each level.
  - Obtain the parameters such as neighbour pixel distance and direction for the gray level co-occurrence matrix.
  - Consider the pixel distance as 1.
  - The four directions (0, 45, 90 and 180, respectively) are considered by this study.
  - The occurrence of the each pixel pair is found and stored in an array.
  - This array is referred to as the ‘co-occurrence matrix’.
  - The mean value is applied on these matrix.
  - These mean values are fed into Support Vector Machine (SVM) for gaining knowledge.
  - Store the gained values for the testing purpose.

Testing phase:

- The testing image which is to be analyzed for stego is obtained.
- Three level counterlet transform is applied on the image.
- The low frequency component of the each level is obtained.
- The parameters neighpour pixel distance and direction for using the gray level co-occurance matrix with pixel distance 1 and 0, 45, 90 and 180, respectively directions are obtained.
- The occurrence of the each pixel pair is found and passed into the array.
- The mean value is applied on the array.
- Now, the gained value of training images and the mean value of the testing image is passed into the Support Vector Machine (SVM) for classification.
- The labelled output classifies between the stego and the normal image.

EXPERIMENTAL ANALYSIS AND RESULTS

This proposed study considers DWT, Ridgelet, Contourlet, Curvelet, Bandelet and Shearlet with respect to first order, run length and GLCM, in order to detect the stego image. Among all the methods Contourlet with GLCM proves 98.79% accuracy in detecting between the normal and the stego image. This percentage is the highest, when it is compared with all the other methods that are shown in Fig. 4.

The misclassification rate, which makes sense that the image that is tested is misclassified as stego while it doesn’t contain any secret message or when it is classified as normal, while actually the image has got some secret embedded message.

This wrong identification is misclassification rate. This study shows a misclassification rate of 1.21, which is the lowest when compared with all other methods and is shown in Fig. 5. The time it takes to complete its processing is somewhat moderate. It consumes time to process an image and is shown in Fig. 6.

The formulae that were used to calculate the detection accuracy, misclassification rate and time consumption is provided below.

The overall detection accuracy is calculated by:

$$Overall\ detection\ accuracy = \frac{No\ of\ detected\ images}{No\ of\ input\ images} \times 100 \quad (11)$$

Misclassification rate is calculated by:

$$Misclassification\ Rule = \frac{No\ of\ correctly\ detected\ images}{No\ of\ input\ images} \times 100 \quad (12)$$

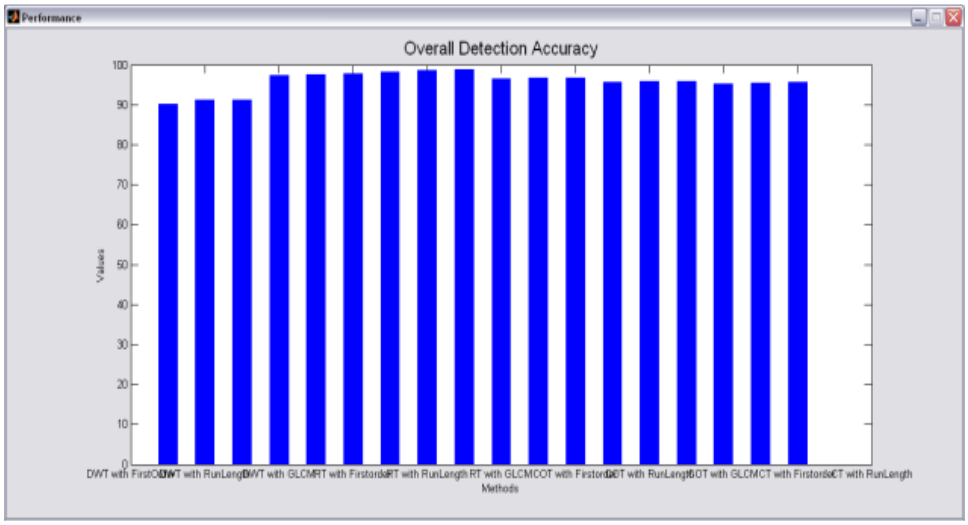

Fig. 4: Overall detection accuracy

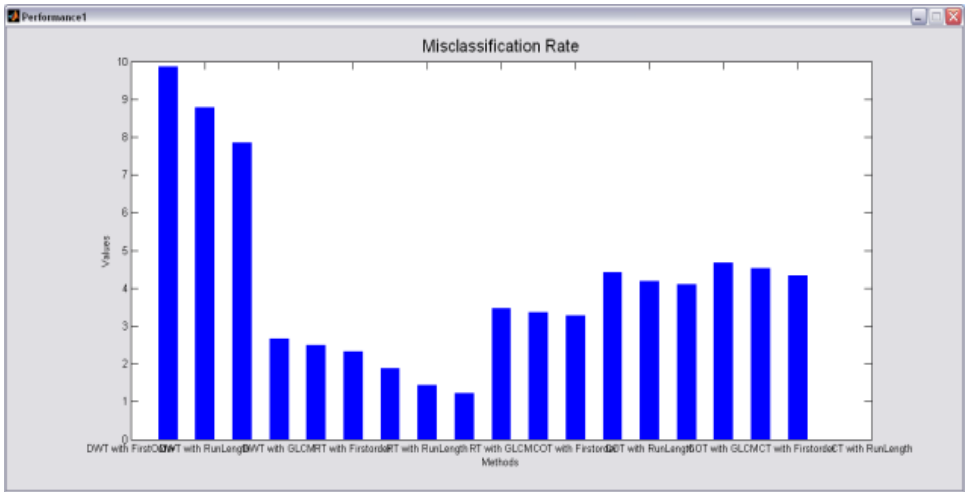

Fig. 5: Misclassification rate

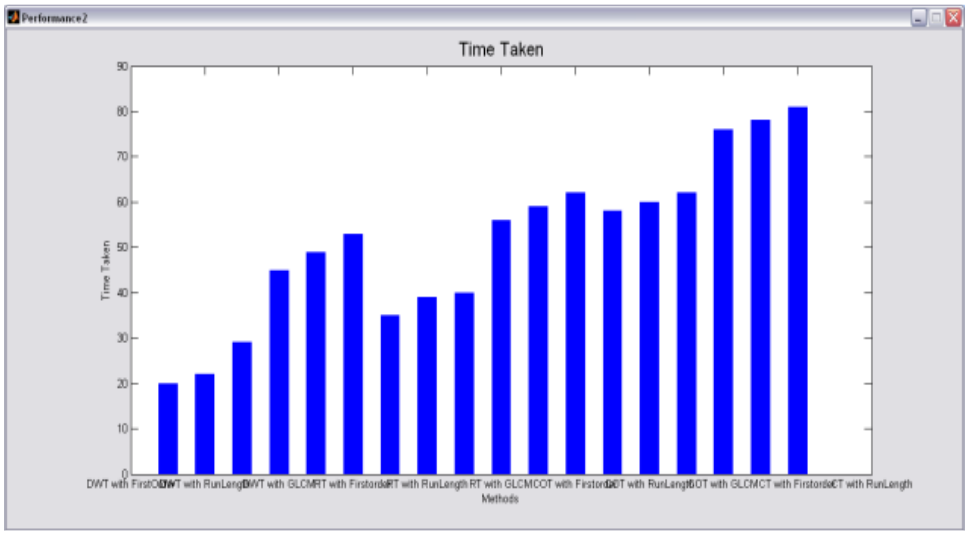

Fig. 6: Time consumption

Table 1: Overall detection accuracy

Methods	Overall detection accuracy	Methods	Overall detection accuracy
DWT with first order	90.13	Curvelet with first order	96.54
DWT with run length	91.21	Curvelet with run length	96.65
DWT with GLCM	92.15	Curvelet with GLCM	96.73
Ridgelet with first order	97.35	Bandelet with first order	95.58
Ridgelet with run length	97.52	Bandelet with run length	95.82
Ridgelet with GLCM	97.68	Bandelet with GLCM	95.91
Contourlet with first order	98.13	Shearlet with first order	95.32
Contourlet with run length	98.57	Shearlet with run length	95.48
Contourlet with GLCM	98.79	Shearlet with GLCM	95.67

Table 2: Misclassification rate

Methods	Misclassification rate	Methods	Misclassification rate
DWT with first order	9.87	Curvelet with first order	3.46
DWT with run length	8.79	Curvelet with run length	3.35
DWT with GLCM	7.85	Curvelet with GLCM	3.27
Ridgelet with first order	2.65	Bandelet with first order	4.42
Ridgelet with run length	2.48	Bandelet with run length	4.18
Ridgelet with GLCM	2.32	Bandelet with GLCM	4.09
Contourlet with first order	1.87	Shearlet with first order	4.68
Contourlet with run length	1.43	Shearlet with run length	4.52
Contourlet with GLCM	1.21	Shearlet with GLCM	4.33

Table 3: Time consumption

Methods	Time taken	Methods	Time taken
DWT with first order	20	Curvelet with first order	56
DWT with run length	22	Curvelet with run length	59
DWT with GLCM	29	Curvelet with GLCM	62
Ridgelet with first order	45	Bandelet with first order	58
Ridgelet with run length	49	Bandelet with run length	60
Ridgelet with GLCM	53	Bandelet with GLCM	62
Contourlet with first order	35	Shearlet with first order	76
Contourlet with run length	39	Shearlet with run length	78
Contourlet with GLCM	40	Shearlet with GLCM	81

Time taken to complete the process is calculated by:

$$Time\ Taken = End\ Time - Start\ Time \quad (13)$$

Corresponding graph for Table 1 is presented in Fig. 4.

Table 2 presents the value of misclassification encountered by each technique and the corresponding graph is presented in Fig. 5. Table 3 deals with the time consumption of every technique and the corresponding graph is shown in Fig. 6.

CONCLUSION

This study shows that the Contouret with GLCM works better than DWT, Ridgelet, Contourlet, Curvelet, Bandelet and Shearlet with its highest accuracy value. Also, every method is tested with respect to first order, run length and GLCM. The misclassification rate is very low in contourlet with GLCM. However, it spares double the time as that of DWT with first order. In future, the time consumption experienced by this study can be minimized.

REFERENCES

Aura, T., 1996. Practical invisibility in digital communication. Proceeding of the 1st International Workshop on Information Hiding, pp: 265-278.

Auria, L. and R.A. Moro, 2008. Support Vector Machines (SVM) as a Technique for Solvency Analysis. DIW Berlin Discussion Paper No. 811.

Chang, C.C. and C.J. Lin, 2001. LIBSVM: A Library for Support Vector Machines 2001 [Online]. Retrieved form: http://www.csie.ntu.edu.tw/~cjlin/libsvm.

Dey, N., A.B. Roy and S. Dey, 2011. A novel approach of color image hiding using RGB color planes and DWT. Int. J. Comput. Appl., 36(5): 19-24.

Farid, H., 2001. Detecting Steganographic message in digital images. Technical Report, TR2001-412, Dartmouth College, New Hampshire, pp: 1-9.

Fontaine, C. and F. Galand, 2009. How Reed-Solomon codes can improve steganographic schemes. EURASIP J. Inform. Secur., 2009: 1-10.

Fridrich, J., 2004. Feature-based steganalysis for JPEG images and its implications for future design of steganographic schemes. Proceeding of the 6th International Information Hiding, Workshop, LNCS 3200, pp: 67-81.

Fridrich, J., M. Goljan and D. Hogea, 2003. Steganalysis of JPEG images: Breaking the F5 algorithm. Proceeding of the 5th International Workshop on Information Hiding, 2578: 310-323.

Fridrich, J., M. Goljan and D. Soukal, 2004. Perturbed quantization steganography with wet paper codes. Proceeding of the ACM Workshop Multimedia and Security. Magdeburg, Germany, pp: 4-15.

Huang, F., J. Huang and Y.Q. Shi, 2012. New channel selection rule for JPEG steganography. IEEE T. Inf. Foren. Sec., 7(4): 1181-1191.

Jassim, D., 2010. Digital Photography and Imaging. SYPEX Inc., Alameda, California, USA, pp: 272.

Jose, T.J.B. and P. Eswaran, 2013. Effective steganalytic algorithm based on residual value of pixels in an image. Int. J. Adv. Comput. Res., 3(12): 32-36.

Kaur, B., A. Kaur and J. Singh, 2011. Steganographic approach for hiding image in DCT domain. Int. J. Adv. Eng. Technol., 1(3): 72-78.

Kundur, D. and D. Hatzinakos, 1998. Digital watermarking using multiresolution wavelet decomposition. Proceeding of the IEEE International Conference Acoustic, Speech, Signal Processing. Seattle WA, pp: 2969-2972.

Schönfeld, D. and A. Winkler, 2007. Reducing the complexity of syndrome coding for embedding. Proceeding of the 9th International Workshop on Information Hiding, 4567: 145-158.

Vaudenay, S., 1996. An Experiment on DES Statistical Cryptanalysis. 3rd ACM Conference on Computer and Communications Security, ACM Press, pp: 139-147.

Westfeld, A., 2001. F5-A Steganographic algorithm: High capacity despite better steganalysis. In: Moskowitz, I.S. (Ed.), Proceeding of 4th International Workshop on Information Hiding (IH'01). Pittsburgh, USA, LNCS 2137, pp: 289-302.

Westfeld, A. and A. Pfitzmann, 2000. Attacks on steganographic systems. In: Pfitzmann, A. (ed.), IH'99. Springer-Verlag, Berlin, Heidelberg, LNCS 1768, pp: 61-75.

Zhu, W., Z. Xiong and Y.Q. Zhang, 1998. Multiresolution watermarking for images and video: A unified approach. Proceeding of International Conference on Image (ICIP'98). Chicago, IL, pp: 465-468.